

# COMPUTING GLOBAL HARMONIC PARAMETERS FOR FLOOD MAPPING USING TU WIEN'S SAR DATACUBE SOFTWARE STACK.

M. Tupas<sup>1,2,\*</sup>, C. Navacchi<sup>1</sup>, F. Roth<sup>1</sup>, B. Bauer-Marschallinger<sup>1</sup>, F. Reuß<sup>1</sup>, W. Wagner<sup>1</sup>

<sup>1</sup>Microwave Remote Sensing Research Group, Department of Geodesy and Geoinformation,  
Technische Universität Wien, Vienna, Austria

(mark.tupas, claudio.navacchi, florian.roth, bernhard.bauer-marschallinger, felix.reuss, wolfgang.wagner) @geo.tuwien.ac.at

<sup>2</sup>Department of Geodetic Engineering, University of the Philippines - Diliman, Quezon City, Philippines

## Commission IV, WG IV/4

**KEY WORDS:** Synthetic Aperture Radar, Data Cube, Harmonic Modeling, Flood Mapping.

### ABSTRACT:

TU Wien's flood mapping algorithm, used for global operations, utilizes harmonic functions to model the seasonal behavior of backscatter to improve flood classification. In earth observation (EO), temporal harmonic models have been used in various scenarios for vegetation and water mapping in the optical and, recently, synthetic aperture radar (SAR) domains. These models condense EO time series stacks to a few Fourier coefficient images that capture seasonal variability, allowing for variable estimation for each day of the year. TU Wien's harmonic parameters consist of these coefficients plus the regression standard deviation and number of observations. However, generating harmonic models at large scales and high resolution presents significant logistical and technical challenges. Particularly for SAR, which requires special handling due to acquisition geometry considerations, implementation on a datacube infrastructure is necessary for agile filtering in metadata, temporal and spatial dimensions. In this work, we highlight our harmonic parameter dataset and our software stack of loosely coupled Python packages, which were deployed in a high-performance computing environment to generate these parameters globally.

## 1. INTRODUCTION

Synthetic Aperture Radar (SAR) backscatter is adept in differentiating standing water due to its low signal compared to most non-water surface cover types. However, the temporal transition from non-water to water is critical to identifying floods. Hence objects with permanent or seasonally low backscatter become ambiguous and difficult to classify. TU Wien's flood mapping algorithm utilizes a pixel-wise harmonic model derived from a Sentinel-1 SAR backscatter datacube [2] at 20 m spatial sampling to account for these patterns. Designed to be applied globally in near-real-time (NRT) [10], the method applies Bayesian inference on Sentinel-1 SAR backscatter data in VV polarization. In this method, the harmonic model generates a non-flooded reference distribution, which is then compared against a flooded distribution to identify flooded pixels within incoming Sentinel-1 scenes.

It is critical for flood mapping workflows, regardless of methods used, to identify reasonable non-flooded backscatter references to distinguish floods from seasonal or permanent inundation. Selecting a previous non-flooded image is an option but is problematic in some cases e.g., long term floods. Another option is to leverage time-series stacks to generate a proxy. Measures of central value such as mean or median are reasonable for areas with slight seasonal variance. However, the majority of the globe show pronounced seasons. Alternatively, moving window versions of such metrics, e.g., rolling three-months-mean, while simple in theory, execution, and seasonally adept, can be resource-intensive, both in recurrent processing and storage. This concern is exacerbated in a global context and when dealing with SAR geometry effects. With this in mind, harmonic (least squares) regression modelling of backscatter time series

was considered for our TU Wien flood mapping algorithm. Harmonic models act as a smoothed proxy for the measurements in the time series, thus allowing for a seasonally varying backscatter reference to be estimated for any given day-of-year using a few pre-computed coefficients.

### 1.1 Harmonic models in earth observation

In earth observation (EO), harmonic models were mainly relevant for vegetation applications in the optical domain so far, e.g., NDVI time series fitting. Harmonic regression models have been shown to effectively capture time-dependent signal patterns from satellite data. This approach assumes seasonality in signal patterns that could be broken down to sinusoidal components attributed to annual, bi-annual, and minor time scale phenomena. One of the most demonstrated use cases of this approach for optical imagery is change detection in vegetation dynamics [? 5]. Others have explored the direct use of harmonic coefficients as parameters to explain and correlate to time-dependent phenomena [8]. Moreover, newer studies show a combination of optical time-series indices and SAR backscatter harmonic parameters improving on this method [14, 9]. The use of SAR data here builds upon the concept that seasonal variations are mainly attributed, but not limited to soil moisture and vegetation dynamics [13], that can be captured by the backscatter time series.

On its own, SAR harmonic models have been used in mapping inundation, and water bodies using Envisat ASAR [13, 12, 11]. These serve as the foundation to our adapted Sentinel-1 flood mapping workflow [1]. It should be noted that investigations in the SAR field are somewhat lacking. Possible hindrances include the unique characteristics of SAR data, such as speckle and acquisition geometry dependence leading to higher complexity in handling its time-series stacks. Hence it is critical

\* Corresponding author.

to have the agility afforded by datacube structures to efficiently perform image stack manipulations such as spatial, temporal, and metadata filtering.

## 1.2 Global coverage

Generating harmonic models at large scales and high resolution presents significant logistical and technical challenges. Therefore, harmonic modelling of remotely sensed time series is often performed on specialized infrastructures [9], such as Google Earth Engine (GEE) [7] or other highly customized setups [17], where the pixel-wise analysis of multi-year data requires well-defined I/O, data chunking, and parallelization strategies to generate harmonic coefficients in reasonable time and cost. While harmonic analysis is not new, to our knowledge, production and application at a global scale using dense SAR time series have yet to be implemented, let alone operationally utilized.

To prepare for a global near real-time flood mapping effort, harmonic coefficients were systematically computed using a global datacube organizing Sentinel-1 SAR backscatter. In the datacube structure, individual images are stacked, allowing for data abstraction in the spatial and temporal dimensions, making it ideal for agile time-series analysis. Nonetheless, for this abstraction to be realized, a rich set of software solutions is needed to implement the 3-dimensional data model.

## 1.3 Objectives

In the following, we present our SAR datacube software stack Figure 1 and its utilization to compute the aforementioned global harmonic parameters. We use a set of portable and loosely coupled Python packages developed by the Research Unit Remote Sensing at the Department of Geodesy and Geoinformation (GEO) at TU Wien, capable of forming a global datacube with minimal overhead from individual satellite images. The stack includes, among others, open-source packages for:

- *yeoda* - for high-level data cube abstraction: <https://github.com/TUW-GEO/yeoda>,
- *Equi7grid* - spatial reference and hierarchical tiling system: <https://github.com/TUW-GEO/Equi7Grid>,
- *veranda* - lower-level data access and I/O: <https://github.com/TUW-GEO/veranda>,
- *geopathfinder* - for spatial file- and folder-based naming and handling: <https://github.com/TUW-GEO/geopathfinder>, and
- *medali* - product tagging and metadata management: <https://github.com/TUW-GEO/medali>.

## 2. HARMONIC PARAMETERS

Before delving into the software and workflow, we describe the product we have produced globally and its formulation. Harmonic models in EO literature are derived from some form of regression of the time series measurements to that of a series of harmonics or sinusoidal components, e.g., Fourier series decomposition. Harmonics could be expressed either as two amplitudes of both sine and cosine components or one amplitude and a phase. Apart from this, differences in their model formulation are the inclusion [15] or non-inclusion [13] of a linear trend component, and the degree of harmonics or the number of iterations the sinusoidal components are repeated in the series,

often referred to as the  $k$  parameter.  $k$  values are usually 2 or 3; higher  $k$  values are avoided to prevent capturing short time scale phenomena attributed to temporary signal changes and effects such as flooding.

In our flood mapping method, a seven coefficient formulation was adopted [13] and is from here on referred to as our harmonic parameters (HPARs). Our HPARs include the backscatter mean and three iterations of two sinusoidal coefficients. The trend component is neglected, and degree of ( $k = 3$ ), where  $c_i$  and  $s_i$  represent the harmonic coefficients,  $\sigma^0$  is the effective mean radar backscatter and  $\hat{\sigma}^0(t)$  is the estimated radar backscatter at time  $t$ .

$$\hat{\sigma}^0(t) = \sigma^0 + \sum_{i=1}^k \left\{ c_i \cos \frac{2\pi it}{n} + s_i \sin \frac{2\pi it}{n} \right\} \quad (1)$$

As described in detail in [2], a non-flooded reference probability distribution function (PDF) is generated for our Bayesian inference, where the estimated backscatter for the day-of-year is used as the mean of the distribution. To build this PDF an assumption of normality and homoscedasticity was imposed to be able to infer the standard deviation from the time-independent sum of square errors (SSE) of the residuals between the pixel's actual time-series and the estimated values (from the harmonic model), divided by the model's degrees of freedom (ref. Eq. 2).

$$std(\sigma_\rho^0) = \sqrt{\frac{SSE}{n - (2k + 1)}} \quad (2)$$

Thus  $\sigma_\rho^0$  is included along with the regression coefficients. For quality assurance purposes,  $n$  or the number of observations is also stored to complete our parameter set.

### 2.1 Product description

For the NRT flood mapping operations, these parameter sets are stored as individual GeoTIFF files. The HPARs files are named in consistency with our datacube's file naming convention similar to [1]. In the case of our HPAR processing, we utilize the *yeoda* file naming convention, defined in the *geopathfinder* package, which allows for files to be read and abstracted, similar to the pre-processed datacube containing backscatter data. For brevity, the readers are directed to the source code<sup>1</sup> for the individual meta information contained in the *yeoda* file naming scheme. This naming scheme includes placeholders for the product name (HPARs) and parameter name encoded as follows:

- **M0** - effective mean of the time series stacks, equivalent to  $\sigma^0$  in Eq. 1, also called the harmonic residual in other literature [8]
- **Cn** - cosine component coefficients, equivalent to  $c_i$  in Eq. 1
- **Sn** - sine component coefficients, equivalent to  $s_i$  in Eq. 1
- **STD** - standard deviation of residual computed by Eq. 2, a proxy for goodness of fit
- **NOBS** - number of observations used for the least squares regression, also an indicator solution quality.

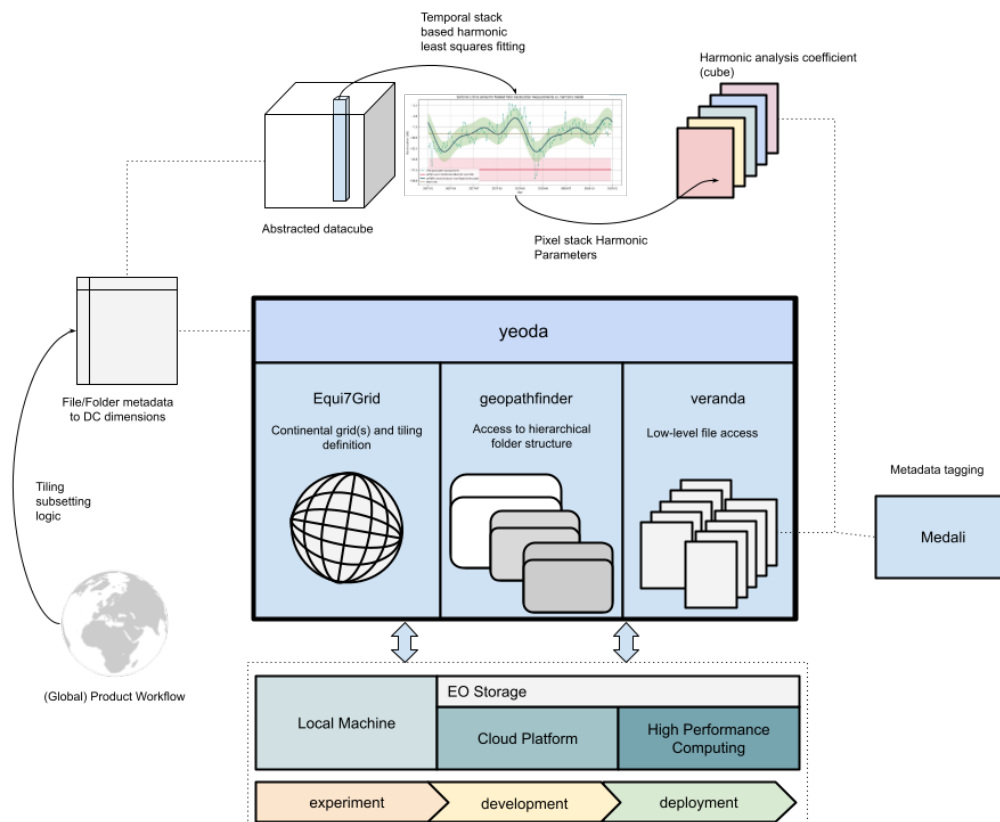


Figure 1. Overview of TU Wien datacube software stack for HPAR computations.

Sample HPAR subsets for two selected regions are shown in Figure 2 covering areas within Mexico and the United Kingdom. The **M0** parameters have value ranges similar to that of the observed backscatter scenes, while all subsequent harmonics have a range of not more than -2.5 dB to 2.5 dB. In the same figure, it can be observed that some land cover types e.g., vegetation and water, have distinct responses to specific parameters where **Cn** parameters seem to be positively related to vegetation. In contrast, for the selected areas seasonal water changes are related to **Sn** parameters. The generated four day-of-year (DoY) expected values for the two sites also show consistency with the documented climate for these areas, as referenced from the work of [4]. The region of interest in Mexico in row three shows greater variation in water as expected of a tile with a predominantly tropical climate with a monsoon. On the other hand, the UK tile in the temperate climate, with no dry season and warm summer, shows larger seasonal vegetation variance. Consistent with [8], the parameters show decreasing information contribution as  $k$  gets larger. Thus increasing  $k$  value further has a diminishing value, validating our  $k = 3$  selection.

### 3. PRODUCT GENERATION

As previously described, generating the parameters was a significant endeavour, requiring an extensive processing infrastructure and the software to support it. Processing of the HPAR products was executed on the Vienna Scientific Cluster (VSC)<sup>2</sup>. The detailed description of the pre-processing and storage infrastructure used for the global datacube is outlined by [16]. Here,

<sup>1</sup> [https://github.com/TUW-GEO/geopathfinder/blob/master/src/geopathfinder/naming\\_conventions/yeoda\\_naming.py](https://github.com/TUW-GEO/geopathfinder/blob/master/src/geopathfinder/naming_conventions/yeoda_naming.py)

<sup>2</sup> <https://vsc.ac.at>

we focus on the processing workflow and software interfaces.

Computing the large-scale product from the ground up required experimentation with viable HPAR formulations, time-series pre-processing steps, and chunking and tasking strategies. However, direct development in an HPC environment is cumbersome, if not wasteful of resources. It was thus critical to be able to perform time-series experiments across different platforms while working on the same level of abstraction regardless of the scale in the temporal and spatial dimensions. The initial experiments were done at small scale, both spatially and temporally, on off-the-shelf machines being suitable for this purpose. Once the desired formulation and strategy were agreed upon, the development of HPC scripts was undertaken. In this step, it was critical to simulate the expected environment of an HPC. Thus, this was performed on a cloud platform (OpenStack<sup>3</sup> environment) that shares the whole pre-processed datacube storage with the HPC, minimizing issues when deploying the HPC processing tasks. Through out this process, it was crucial that our datacube access and processing methods remained consistent regardless of the platform. Hence the need for software that can abstract datacubes from a collection of files regardless of their location. For this purpose, we present our software stack.

#### 3.1 SAR datacube software stack

Interfaces of the packages and the software objects contained are shown in Figure 3. The red classes in the diagram show the HPC scripts driving the tasking and operation, the yellow classes are the *NumPy* arrays used for the computations (*xarray*

<sup>3</sup> <https://www.openstack.org/>

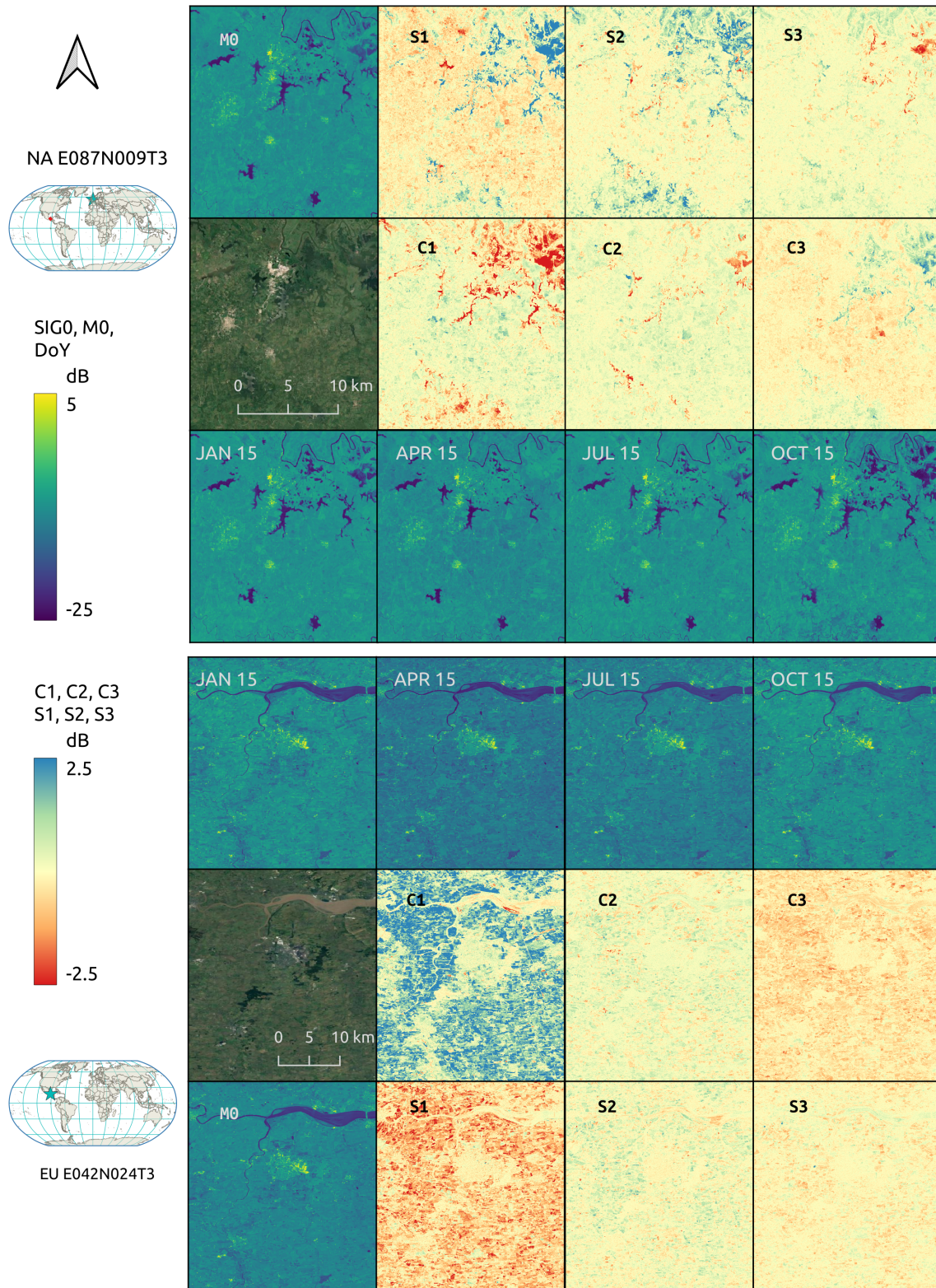


Figure 2. Sample HPARs and day-of-year (DoY) estimates

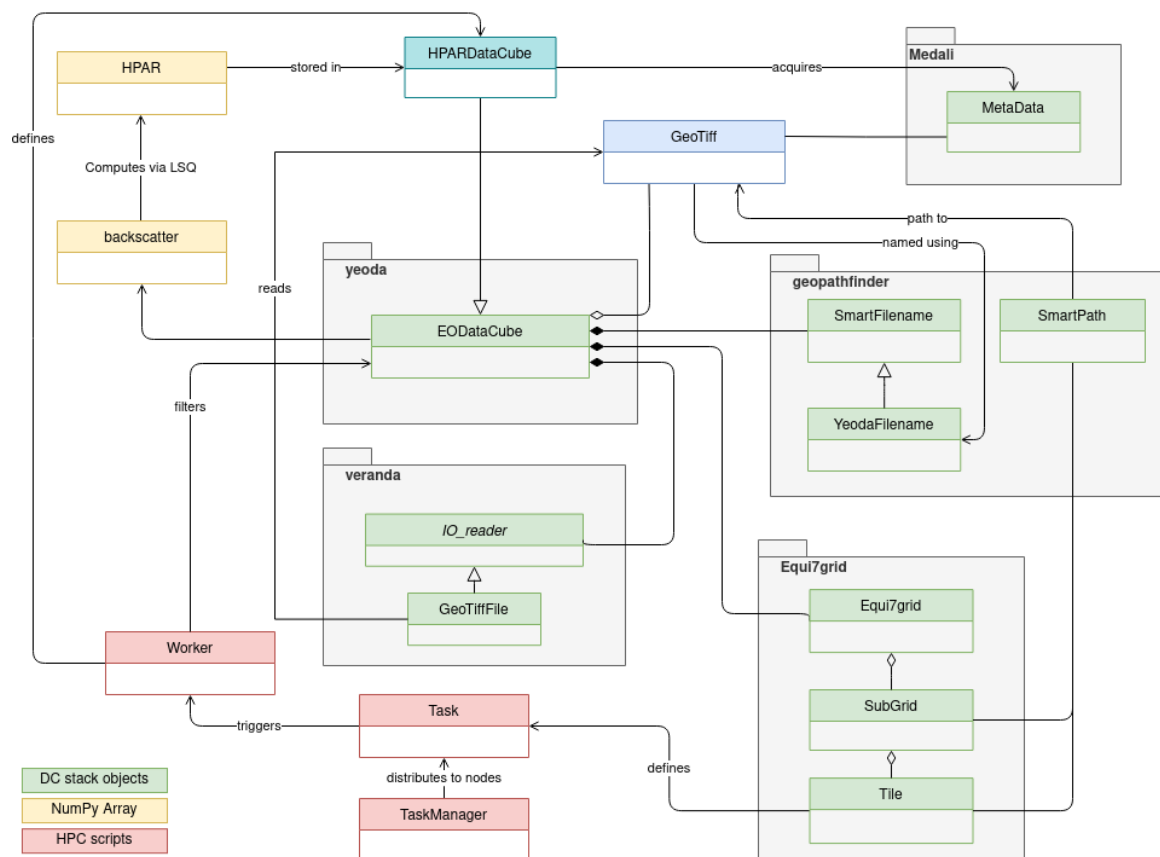


Figure 3. SAR datacube software stack and HPAR class diagram

classes can also replace these), while the green classes are those from the collection of packages described herein.

Working from the pre-processed SAR backscatter datacube, the logical entry point is through *yeoda*, which stands for 'your Earth Observation Data Access'. *yeoda* abstracts well-structured EO data collections as a datacube, making high-level operations such as filtering and data loading possible. This level of abstraction is supported by the other components of the software stack, which address the organization and lower-level access to individual files. This structure is shown in Figure 3, where an *EODataCube* — our basic datacube class — plays a central role in the software ecosystem where it requires a defined projected grid system (e.g., *Equi7Grid*), low-level data readers and writers (e.g., *GeoTiffFile*), file naming (e.g., *YeodaFileName*) and file path/folder tree definitions (e.g., *SmartFile-path/SmartTree*). In the context of the HPAR processing, the GeoTIFF file format was selected for input and output. However, *yeoda* is also capable of reading and writing NetCDF data.

From a data storage perspective, our SAR backscatter datacube is simply a collection of raster datasets in GeoTIFF file format co-registered in the same reference grid. To deploy for large-scale operations, a well-defined grid system must deal with high-resolution raster data. A tiling system fulfilling this requirement is the *Equi7grid*, based on seven equidistant continental projections found to minimize raster image oversampling [3]. *Equi7grid* hierarchy is composed of continental grids and subsequent tiles contained therein. Here several tile definitions are possible. In the case of the NRT flood mapping, 'T3' tiles composed of 15000 x 15000 pixels with 20 m pixel spacing are used. Interacting with this tiling system on an abstract level is possible via our in-house developed *Equi7Grid* package.

The tiling system follows a hierarchy of directories to manage the datasets on disk. Moreover, for individual files, a pre-defined naming convention is applied to indicate spatial, temporal, and ancillary information from product metadata that becomes transparent to *yeoda*. This setup of customizable file naming schemes is easily managed through the *geopathfinder* package. We utilize the so called *YeodaFileName* class, which pre-defines a set of file name entries and their respective encoders and decoders, as described in the product definition for this endeavour. However, other file naming schemes previously utilized for other projects are also available as subclasses of the *SmartFilename* class being extensible to match processing and naming requirements.

In the context of the HPAR computations, easy filtering and subsetting of the SAR datacube was an integral functionality provided by *yeoda*. The actual HPARs processing task was subdivided into multiple HPC jobs on the VSC based on the presented tiling and folder hierarchy given by the *Equi7Grid*. For the temporal domain modelling to work, data is further split into manageable chunks. Thus only one tile per HPC node was allocated. *yeoda* was then used to filter the datacube by various spatiotemporal dimensions, and also dimensions including metadata information on the SAR viewing geometry, i.e. the relative orbit.

On the lower level, a three-dimensional *NumPy* array of decoded backscatter measurements was generated by *veranda* from the image stack on disk. *veranda*, which stands for 'vector and raster data access', is a package that wraps input and output functionality. *Veranda* aims to provide the core interface between higher level datacubes and the data on disk. This is intended to give performant data access for *yeoda* which would

later on include parallelism in write and read access. In the current use case, access to stacks of GeoTIFF files is currently done via *GDAL*<sup>4</sup> in the background.

Due to the depth of the datacube, further manually initiated segmentation and parallelization were required at this level. Thus, pixel-based parallelization was done using *Numba*<sup>5</sup> to handle the core least squares estimation of the measurements versus a day-of-year array derived from image timestamps. *veranda* is again used for the output operation to encode and write the HPARs to individual files. After data quality checks, which are done using an external package, the metadata encoding is performed via *medali* and caps the processing. The output files were also named and stored using the *YeodaFileName* convention. In this manner, the HPAR product themselves can be abstracted as a multi-dimensional datacube and simplify subsequent flood mapping computations.

### 3.2 HPC processing

Unlike ENVISAT ASAR data used in the case of Schlaffer's work [13], where acquisitions at multiple incidence angles at a broad range allow for backscatter normalization, Sentinel-1 data is being acquired at a narrow range of incidence angles. However, Sentinel-1 has a more systematic acquisition plan with two satellites orbiting at regular intervals resulting in return cycles of six days in higher latitudes and 12 days near the equator. Albeit done per orbit direction and relative orbit number, this still provides a large set of samples to which the least-squares regression could be applied, except for a few tiles where artefacts are observed due to the low number of samples.

The harmonic model was generated globally for each T3 Equi7grid tile as represented by its regression parameters sets. To account for incidence angle dependence, computations were done per relative orbit. Thus the seven parameter set, plus standard deviation and number of observations, are stored operationally per pixel per relative orbit.

A description of the HPARs generation steps that were performed on the VSC, using custom Python scripts optimized for parallelization at both tile level (inter node) and pixel-based computation (intra node), metadata generation, and quality checking, is enumerated here:

1. tasks are distributed to multiple nodes based on predefined jobs. In this case, jobs were started per sub-grid, where each task can be a single tile or smaller depending on the depth of the stack at that location
2. for each task, a datacube subset is instantiated using the Equi7grid sub-grid (continent) and its tile name.
3. the datacube is then filtered to include only the date range specified and VV polarized backscatter data
4. individual processes are started from subsequently filtered datacubes per relative orbit number
5. parallel computation of harmonic regression for each temporal pixel stack in the tile
6. after disregarding no data records at each pixel stack, each backscatter measurement and corresponding timestamp converted to a day-of-year are included in the samples
7. least squares regression is performed at each stack, where the number of observations is noted per pixel, and the sum of square errors (SSE) is used to compute the standard deviation
8. parameters with number of observations and standard deviations are encoded and compressed to individual GeoTIFF files
9. quality checking is performed per file to check for I/O errors or data range issues
10. metadata and log files are generated in a final step

All log files and random GeoTIFF file samples were parsed and rechecked for consistency. Failed parameter sets were rerun until all issues have been resolved. In all, 110,115 files for the 12,235 tile-orbit sets with a total size of 9.9 TB were generated using data from 2019 and 2020. The spatial distribution of the generated HPARs is shown in Figure 4 as represented by the **M0** parameter. The coverage map was cross-checked against Sentinel-1 Global Backscatter Model (SIGBM) data that covers 96.5% of land surface outside of Antarctica [1]. It was noted that a few tiles show artefacts indicating ill-fitting regression in small regions in Asia, Africa, and North America, corresponding areas with low Sentinel-1 data availability.

## 4. SUMMARY AND CONCLUSIONS

In this contribution, we described a global Sentinel-1 harmonic parameter dataset and its computation on the VSC, using an open-source software stack that takes hierarchically structured tiles and provides reading, writing, and processing abstraction as a functional datacube. With the HPAR dataset, the Sentinel-1 time series was seasonally modelled from 2019 to 2020 and condensed to a fraction of the size of the original global backscatter datacube. While, for now, it is exclusively used to allow our flood monitoring workflow to work globally in near-real-time, other potential applications include seasonal water and vegetation analysis.

### 4.1 Possible use cases

Inundation mapping is expected to be the primary use case of the above-described dataset with the data generated in the VV polarization. In this regard, seasonal water body mapping is an obvious use case shown in the Mexico study site above. Aside from the flood mapping and water body mapping potential described, the global parameter set could have potential use for vegetation such as forestry or change detection. However, conversion to amplitude and phase formulation might be needed [8] as most derived harmonic parameters use composite amplitude or phase values. These use cases could similarly be extended in tandem with optical images for vegetation and change detection analysis [9, 14].

On the other hand, seasonality parameters similar to [6] derived from time series which indicates the start of season, end of season, length of season, and amplitude could potentially be directly extracted from the harmonic model rather than iterating through a full time series. The harmonic model would serve as a temporally smoothed value from observed values, thus potentially being easier to use in phenological studies.

<sup>4</sup> <https://gdal.org/>

<sup>5</sup> <https://numba.pydata.org/>

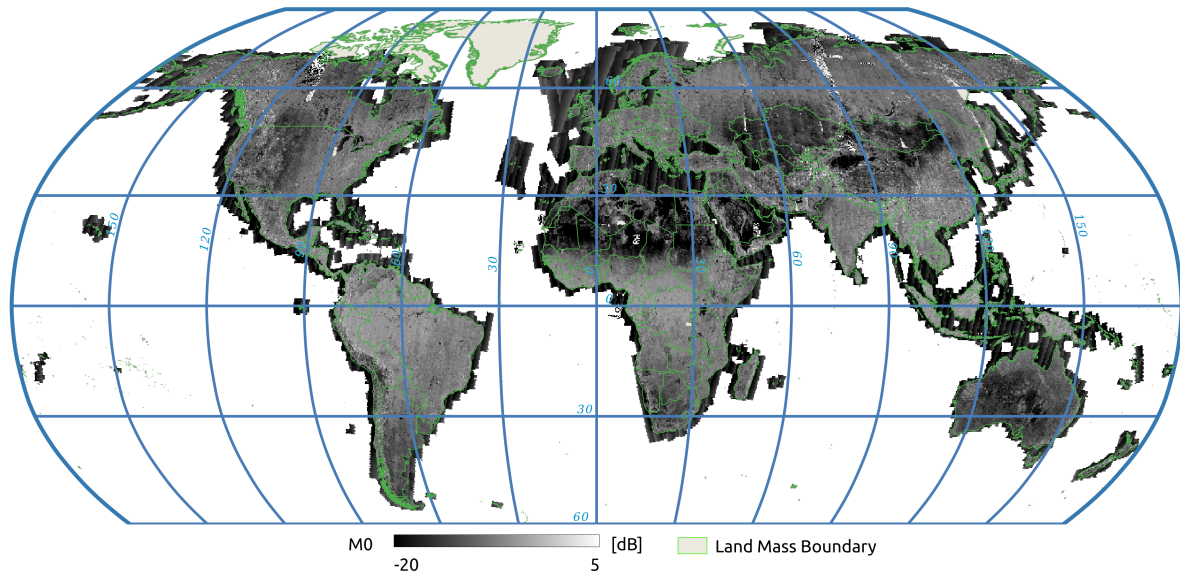


Figure 4. Global coverage map of HPARS - M0

## 4.2 Software stack outlook

As described in Figure 3, the generated HPARs use the same storage scheme and thus can also be accessed as a datacube. The same approach was used in the ongoing NRT flood processing, where the presented software stack is operationally applied in dedicated cloud-based platforms — demonstrating the portability of the loosely coupled packages. This shows that our software stack can be deployed on different platforms with little to no overhead, underlining the tremendous potential of reproducible datacube analysis at small or large scales. From our experience, the stack provides the essential tools for analyzing high resolution datacubes for experimental analysis to large scale time sensitive operations. The opensource license of the software components allows for reproduction in environments with different filenames, storage, and processing requirements.

As of this writing, the packages are in active development, where improved parallelism in reading and writing of datacubes is in the pipeline.

## ACKNOWLEDGEMENTS

This work was partly funded by TU Wien, with co-funding from the project "Provision of an Automated, Global, Satellite-based Flood Monitoring Product for the Copernicus Emergency Management Service" (GFM), Contract No. 939866-IPR-2020 for the European Commission's Joint Research Centre (EC-JRC), and the project "Flood Event Monitoring and Documentation enabled by the Austrian Sentinel Data Cube" (ACube4Floods), Contract No. 878946 for the Austrian Research Promotion Agency (FFG, ASAP16).

The computational results presented have been achieved using the Vienna Scientific Cluster (VSC). We further would like to thank our colleagues at TU Wien and EODC for supporting us on technical tasks to cope with such a large and complex dataset.

## References

- Bauer-Marschallinger, B., Cao, S., Navacchi, C., Freeman, V., Reuß, F., Geudtner, D., Rommen, B., Vega, F. C., Snoeij, P., Attema, E., Reimer, C., Wagner, W., 2021. The normalised Sentinel-1 Global Backscatter Model, mapping Earth's land surface with C-band microwaves. *Scientific Data*, 8(1), 277.
- Bauer-Marschallinger, B., Cao, S., Tupas, M. E., Roth, F., Navacchi, C., Melzer, T., Freeman, V., Wagner, W., 2022. Satellite-Based Flood Mapping through Bayesian Inference from a Sentinel-1 SAR Datacube. *Remote Sensing*, 14(15), 3673. <https://www.mdpi.com/2072-4292/14/15/3673>.
- Bauer-Marschallinger, B., Sabel, D., Wagner, W., 2014. Optimisation of global grids for high-resolution remote sensing data. *Computers & Geosciences*, 72, 84–93.
- Beck, H. E., Zimmermann, N. E., McVicar, T. R., Vergopolan, N., Berg, A., Wood, E. F., 2018. Present and future Köppen-Geiger climate classification maps at 1-km resolution. *Scientific Data*, 5(1).
- Chen, J., Chen, J., Liu, H., Peng, S., 2018. Detection of Cropland Change Using Multi-Harmonic Based Phenological Trajectory Similarity. *Remote Sensing*, 10(7), 1020.
- Csorba, A., Szegi, T., Fodor, H., Bukombe, B., Uwiragiye, Y., Naramabuye, F. X., Michéli, E., 2019. Characterization of rice agriculture in the Southern Province of Rwanda by means of microwave remote sensing. *Physics and Chemistry of the Earth, Parts A/B/C*, 112, 58–65.
- Gorelick, N., Hancher, M., Dixon, M., Ilyushchenko, S., Thau, D., Moore, R., 2017. Google Earth Engine: Planetary-scale geospatial analysis for everyone. *Remote Sensing of Environment*, 202, 18–27.
- Immerzeel, W. W., Quiroz, R. A., de Jong, S. M., 2005. Understanding precipitation patterns and land use interaction in Tibet using harmonic analysis of SPOT VGT-S10 NDVI time series. *International Journal of Remote Sensing*, 26(11), 2281–2296. <https://doi.org/10.1080/01431160512331326611>.

Liu, X., Zhai, H., Shen, Y., Lou, B., Jiang, C., Li, T., Hus-sain, S. B., Shen, G., 2020. Large-Scale Crop Mapping From Multisource Remote Sensing Images in Google Earth Engine. *IEEE Journal of Selected Topics in Applied Earth Observations and Remote Sensing*, 13, 414–427. Conference Name: IEEE Journal of Selected Topics in Applied Earth Observations and Remote Sensing.

Salamon, P., Mctormick, N., Reimer, C., Clarke, T., Bauer-Marschallinger, B., Wagner, W., Martinis, S., Chow, C., Böhnke, C., Matgen, P., Chini, M., Hostache, R., Molini, L., Fiori, E., Walli, A., 2021. The New, Systematic Global Flood Monitoring Product of the Copernicus Emergency Management Service. *2021 IEEE International Geoscience and Remote Sensing Symposium IGARSS*, 1053–1056. ISSN: 2153-7003.

Schlaffer, S., Chini, M., Dettmering, D., Wagner, W., 2016. Mapping wetlands in Zambia using seasonal backscatter signatures derived from ENVISAT ASAR time series. *Remote Sensing*, 8(5).

Schlaffer, S., Chini, M., Giustarini, L., Matgen, P., 2017. Probabilistic mapping of flood-induced backscatter changes in SAR time series. *International Journal of Applied Earth Observation and Geoinformation*, 56, 77–87.

Schlaffer, S., Matgen, P., Hollaus, M., Wagner, W., 2015. Flood detection from multi-temporal SAR data using harmonic analysis and change detection. *International Journal of Applied Earth Observation and Geoinformation*, 38, 15–24.

Shimizu, K., Ota, T., Mizoue, N., 2019. Detecting Forest Changes Using Dense Landsat 8 and Sentinel-1 Time Series Data in Tropical Seasonal Forests. *Remote Sensing*, 11(16), 1899. <https://www.mdpi.com/2072-4292/11/16/1899>.

Verbesselt, J., Zeileis, A., Herold, M., 2012. Near real-time disturbance detection using satellite image time series. *Remote Sensing of Environment*, 123, 98–108.

Wagner, W., Bauer-Marschallinger, B., Navacchi, C., Reuß, F., Cao, S., Reimer, C., Schramm, M., Briese, C., 2021. A Sentinel-1 Backscatter Datacube for Global Land Monitoring Applications. *Remote Sensing*, 13, 4622.

Zhou, J., Jia, L., Menenti, M., Liu, X., 2021. Optimal Estimate of Global Biome—Specific Parameter Settings to Reconstruct NDVI Time Series with the Harmonic ANalysis of Time Series (HANTS) Method. *Remote Sensing*, 13(21), 4251.